

Planning of Survivable Wavelength-Switched Optical Networks based on P2MP Transceivers

Yuxiao Zhang, Qian Lv, Ruoxing Li, Xiaojian Tian, and Zuqing Zhu, *Fellow, IEEE*

Abstract—Nowadays, the booming of emerging network services have shifted the major traffic pattern in metro-aggregation networks from point-to-point (P2P) to hub-and-spoke (H&S). Hence, it will be promising to plan metro-aggregation networks with point-to-multipoint coherent optical transceivers (P2MP-TRXs). This work studies how to plan a survivable wavelength-switched optical network (WSON) with P2MP-TRXs and shared backup path protection (SBPP) to address single-link failures. We formulate an integer linear programming (ILP) model to place P2MP-TRXs, assign sub-carriers (SCs) to P2MP-TRXs, and calculate routing and spectrum assignment (RSA) for the working/backup lightpath between each hub-leaf P2MP-TRX pair, such that traffic demands can be satisfied with the minimum cost. A heuristic based on adaptive demand grouping (ADG) is also proposed to solve the problem time-efficiently. Extensive simulations confirmed the performance of our proposals.

Index Terms—Wavelength-switched optical networks, Point-to-multipoint transceivers, Survivable network planning, Shared backup path protection.

I. INTRODUCTION

COMMUNICATION service providers (CSPs) are always trying to reduce the capital expenditures (CAPEX) and operating expenses (OPEX) of service delivery for better economic benefits. With the fast development of cloud computing, data-center networks (DCNs) and Internet-of-Things (IoT), CSPs have to look for new technologies continuously to cope with the explosive growth of network services and data traffic, especially for the metro-aggregation segments [1–4]. This has led to many innovations, such as flexible-grid elastic optical network (EON) [5–9] and coherent optics [10], to make the underlying optical infrastructure of the Internet more adaptive and cost-effective. Meanwhile, emerging network services lead to large amounts of in-cast (many-to-one) and multicast traffic [11], shifting the major traffic pattern from point-to-point (P2P) to hub-and-spoke (H&S) [12], and thus have promoted the research and development (R&D) on point-to-multipoint (P2MP) coherent optical transceivers (P2MP-TRXs) [13].

Note that, to support H&S traffic, a hub node needs to talk with a set of leaf nodes simultaneously, while the data-rates between different hub-leaf pairs might not be the same [14]. Fig. 1 shows the difference between provisioning H&S traffic with P2P transceivers (P2P-TRXs) and P2MP-TRXs. For the scheme in Fig. 1(a), we need to deploy a number of P2P-TRXs in pairs at the hub and leaf nodes. This not only results in the need for many TRXs and router interfaces but also complicates

the network control and management (NC&M) [15]. On the other hand, the optical grooming realized by P2MP-TRXs can better adapt to the H&S traffic between the hub and leaf nodes. Specifically, as shown in Fig. 1(b), we place a high-capacity hub P2MP-TRX to communicate with multiple low-capacity leaf P2MP-TRXs, enabling the interoperability between TRXs operating at different data-rates [15]. Hence, the CAPEX due to TRXs can be reduced together with router port usages.

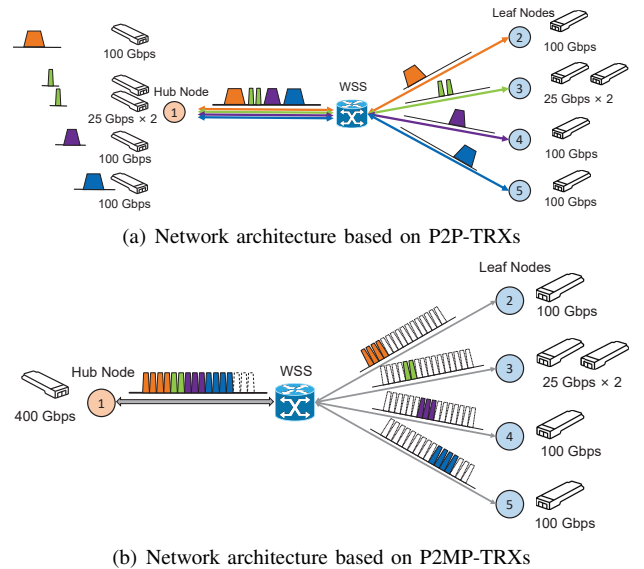


Fig. 1. Examples on provisioning H&S traffic with P2P-TRXs and P2MP-TRXs, WSS: wavelength-selective switch.

The invention of P2MP-TRXs can be traced back to the multiflow transponders proposed in [14]. Recently, by leveraging digital subcarrier modulation (DSCM), researchers have designed a novel type of P2MP-TRXs, each of which can generate a set of low-speed Nyquist sub-carriers (SCs) to slice a wavelength channel for fine-granularity spectrum allocations [16]. For instance, a 400-Gbps hub P2MP-TRX can divide its capacity into 16 SCs, each of which uses 4 GHz to achieve 25 Gbps with dual-polarization and 16 quadrature amplitude modulation (DP-16QAM), and the SCs can be allocated to the connections to different low-speed leaf P2MP-TRXs [13]. The most attractive benefit of this type of P2MP-TRXs is that each of them has similar complexity and cost as those of a P2P-TRX operating at the same maximum data-rate [17].

The aforementioned studies only considered to deploy P2MP-TRXs in relatively simple topologies that are physically correlated to H&S traffic (*e.g.*, horseshoe and tree topologies). However, we hope to point out that there are a few advantages

Y. Zhang, Q. Lv, R. Li, X. Tian, and Z. Zhu are with the School of Information Science and Technology, University of Science and Technology of China, Hefei, Anhui 230027, P. R. China (email: zqzhu@ieee.org).

Manuscript received on November 14, 2022.

of applying P2MP-TRXs in metro-aggregation networks with mesh topologies [18]. First, a mesh topology can also carry H&S traffic well because it can usually be decomposed into a set of horseshoe or tree topologies. Second, mesh topologies usually have better connectivity, and thus they can provide higher survivability during link/node failures. Finally, due to their flexibility, mesh topologies can adapt to dynamic H&S traffic demands better, such as the number of leaves to a hub changes dynamically during network operation.

Although the P2MP-TRXs have a good prospect for being deployed in metro-aggregation networks to support H&S traffic, the network planning and provisioning with them have just started to attract research interests [12, 19, 20] and existing studies in this field were all based on the filterless optical network (FON) [21], where communications are realized with the broadcast-and-select scheme in fiber trees. Note that, even though P2MP-TRXs and FONs are naturally compatible [12] and the combination of them can indeed bring in appealing cost-efficiency [19], the drawbacks are also noticeable. First of all, to avoid laser-loops, FONs should be architected with loopless fiber trees [22], which applies strict topology restrictions on network planning and can result in poor reconfigurability during network provisioning. Second, due to the broadcast-and-select scheme, an FON will broadcast the whole spectrum from a hub P2MP-TRX to all the nodes in its fiber tree, which can result in a significant amount of spectrum waste.

Therefore, it would be interesting and relevant to study the applications of the P2MP-TRXs in optical networks other than FONs, for improved reconfigurability and spectrum-efficiency. Note that, there are a number of optical filtering techniques based on which SC-level sub-wavelength switching can be realized. For example, the SC-level sub-wavelength switching based on fiber Bragg gratings (FBGs) has been demonstrated decades ago [23, 24], and commercial wavelength-selective switches (WSS') based on liquid-crystal-on-silicon also have such capability [25]. However, to the best of our knowledge, the network planning and provisioning of wavelength-switched optical networks (WSONs) with P2MP-TRXs have not been considered in the literature yet, and more importantly, they are more challenging than their counterparts for FONs.

For instance, to plan a WSON, we need to deploy P2MP-TRXs, assign SCs to P2MP-TRXs, and calculate the routing and spectrum assignment (RSA) of each lightpath between a hub-leaf P2MP-TRX pair, for satisfying certain traffic demands. The fundamental differences between FON and WSON determine that the algorithms designed for planning FONs with P2MP-TRXs cannot be leveraged to solve similar network planning problems related to WSONs, especially for the RSA part. Specifically, the broadcast-and-select scheme makes the RSA in P2MP-TRX-based FONs relatively simple, but the RSA in P2MP-TRX-based WSONs is rather complex. As shown in Fig. 1(b), each set of hub and leaf P2MP-TRXs are interconnected by a light-tree, where the spectrum assignments on the branches are correlated because they are all from the same hub P2MP-TRX. In other words, the spectra assigned on the light-tree's branches should be packed within a fixed spectral range (*i.e.*, the bandwidth used by the hub P2MP-TRX). To the best of our knowledge, such a correlated RSA

can hardly be solved with existing algorithms in the literature.

More importantly, we should not ignore survivability when planning WSONs with P2MP-TRXs, because critical failures can happen everywhere and at any time [26–28]. Meanwhile, as network and resource virtualization is frequently utilized in metro-aggregation networks [29–31], the impacts caused by the failures can even be amplified because the breakdown of a physical device will interrupt all the virtual functions/networks that use it [32]. Nevertheless, planning a survivable WSON with P2MP-TRXs will be more complex, especially when we need to reduce the spectrum usages of backup lightpaths for improving protection efficiency. Previously, researchers have designed numerous protection schemes for EONs, including both path protection [33] and link protection [34], and by leveraging the centralized NC&M of software-defined networking (SDN) [35, 36], fast restoration of lightpaths within a few milliseconds has been demonstrated [37]. However, as all the existing studies in this area did not address the correlated RSA mentioned above, we cannot leverage their approaches to plan survivable WSONs with P2MP-TRXs.

The aforementioned considerations motivate us to study how to plan survivable WSONs with P2MP-TRXs to address single-link failures. To improve the protection efficiency of planned WSONs, this work considers to plan survivable WSONs with shared backup path protection (SBPP). We first formulate an integer linear programming (ILP) model to place P2MP-TRXs, assign SCs to P2MP-TRXs, and calculate RSA for working/backup lightpath between each hub-leaf P2MP-TRX pair, such that a set of traffic demands can be satisfied with the minimum CAPEX. Then, a time-efficient heuristic is proposed to solve large-scale problems quickly. Specifically, we design an adaptive demand grouping (ADG) scheme to group demands such that each group can be mapped to a set of hub-leaf P2MP-TRXs cost-efficiently. The performance of the proposed algorithms are evaluated with extensive simulations. The simulation results confirm that our ADG-based heuristic can approximate the optimal results from the ILP well and outperform greedy-based benchmarks significantly.

The rest of the paper is organized as follows. Section II briefly surveys the related works. In Section III, we describe the network model of the survivable WSON planning with P2MP-TRXs. The ILP model and ADG-based heuristic are presented in Sections IV and V, respectively. In Section VI, we discuss the simulations for performance evaluation. Finally, Section VII summarizes the paper.

II. RELATED WORK

The recent advances on P2MP-TRXs are enabled by DSCM, which leverages Nyquist shaping to get a set of closely packed SCs (*e.g.*, each operates at 4 GBaud [13]) based on a single optical carrier. Hence, the physical-layer impairments due to dispersion and fiber nonlinearity can be mitigated effectively [38]. With DSCM, the SCs from a hub P2MP-TRX can be managed independently to use various modulation formats and send to different leaf P2MP-TRXs [20], and thus the spectrum allocation granularity in WSONs can be further reduced to SC-level (*i.e.*, several GHz and is even smaller than that in EONs).

Therefore, the emergence of DSCM-based P2MP-TRXs has effectively improved the flexibility of optical communications. The P2MP-TRXs have been evaluated in lab testbeds [16] and field trails [39], and the studies in [15, 17] have performed the techno-economic analysis to suggest that P2MP-TRXs will be more cost-effective than P2P-TRXs in long run.

By assuming an FON architecture, researchers have tackled the network planning and service provisioning with P2MP-TRXs in [12, 18–20, 40]. Back *et al.* [12] considered the planning of P2MP-TRX-based FONs with specific topologies, but they did not address the assignments of SCs and spectrum in the optimization model. In [19], the authors studied the multilayer planning to place P2MP-TRXs in the FONs that have fault-tolerant ring topologies, and formulated a mixed ILP (MILP) model to overcome the sub-optimality of their previous algorithm design in [18]. The planning of survivable FONs with P2MP-TRXs was also tackled in [20], where an ILP model was formulated to build link-disjoint fiber trees for protecting against single-link failures. The study in [40] designed an ILP to optimize the dynamic reconfiguration of SCs in a P2MP-TRX-based FON for improving the network’s adaptivity to dynamic traffic demands. As all the aforementioned studies were based on FONs, the approaches developed in them cannot be leveraged to address the problem considered in this work, especially for the subproblem of correlated RSA.

Previously, many efforts have been devoted to improving the survivability of fixed-grid wavelength-division multiplexing (WDM) networks and flexible-grid EONs, including protection design and service restoration. As restoration does not reserve backup resources, it cannot guarantee successful service recovery and can take relatively long recovery time [41, 42]. Therefore, we consider protection in this work. However, since all the studies on protection design in WDM networks and EONs (*e.g.*, [33, 34, 37]) did not address the correlated RSA that is introduced by the operation principle of P2MP-TRXs, we cannot leverage the existing approaches to plan survivable WSONs with P2MP-TRXs. In all, to the best of our knowledge, the problem of how to plan survivable WSONs with P2MP-TRXs has not been considered in the literature yet.

III. PROBLEM DESCRIPTION

In this section, we describe the network model of P2MP-TRX-based WSONs and the survivable planning for them.

The topology of a WSON is denoted as a graph $G(V, E)$, where V and E are the set of nodes and links, respectively. Different from the case in an FON, each node $v \in V$ contains an optical switch that can realize SC-level sub-wavelength switching. The capacities of hub and leaf P2MP-TRXs are respectively represented by sets O_h and O_l . Here, O_h and O_l partially overlap as $O_h \cap O_l \neq \emptyset$, because certain medium-speed P2MP-TRXs can work as both hub and leaf [13].

In order to plan a survivable WSON based on P2MP-TRXs whose services will be intact during any single-link failure, we need to determine the deployment of P2MP-TRXs on each node $v \in V$, assign SCs to the P2MP-TRXs, and solve the correlated RSA for establishing working/backup lightpaths with SBPP to connect the deployed P2MP-TRXs, such that

all the traffic demands are satisfied. In this work, we consider the H&S traffic pattern, and thus each traffic demand can be modeled with a hub node $h \in V$, a sets of leaf nodes $V_l \subseteq V$, and an array to denote the bi-directional traffic between all the hub-leaf pairs. Hence, by aggregating all the traffic demands, we can obtain a traffic matrix $\mathbf{D} = [d_{h,l}]_{|H| \times |L|}$, where each element $d_{h,l}$ represents the total amount of traffic from a hub h to a leaf l ($h, l \in V$), in terms of the number of required SCs when each SC occupies 4 GHz to provide a capacity of 25 Gbps with DP-16QAM [20], and H and L denote the sets of hub and leaf nodes, respectively ($H \subseteq V, L \subseteq V$).

We assume that the bandwidth of an SC is fixed as 4 GHz, while two modulation formats (*i.e.*, DP-16QAM and dual-polarization quadrature phase-shift keying (DP-QPSK)) can be used by each SC based on its quality-of-transmission (QoT). Specifically, we determine the QoT of a lightpath based on its length, and DP-16QAM can be used if the length of a lightpath does not exceed 500 km, whereas DP-QPSK will be used if the lightpath is longer [15]. The capacities of an SC under DP-QPSK and DP-16QAM are 12.5 Gbps and 25 Gbps, respectively. When considering a network based on Flexible-grid technology (either EON or FON), the spectra on each fiber link $e \in E$ are allocated to lightpaths in frequency slots (FS’), each of which occupies 12.5 GHz, according to the common setup in EONs [5]. In this case, to meet service requirements, the spectrum assigned by a fiber link must be an integer multiple of FS, and should be greater than or equal to the actual bandwidth required by the service. And this can make certain spectrum within an FS unusable. In other words, this spectrum waste exists as long as the optical network operates according to the standardized wavelength grids. If consider a gridless optical network, it is sufficient to allocate spectrum that matches the service’s actual bandwidth requirements. Therefore, when the network is gridless, it indeed can avoid such spectrum waste that exists in the grid-based network.

When assigning the SCs from a hub P2MP-TRX to its leaf P2MP-TRXs, we need to make sure: 1) the SCs allocated to different leaf P2MP-TRXs do not overlap, and 2) all the allocated SCs can only vary within the bandwidth used by the hub P2MP-TRX. Then, for the lightpath between each pair of hub-leaf P2MP-TRXs, we should allocate enough FS’ to carry the SCs used by them. Therefore, the survivable network planning basically consumes two types of resources that are variable, *i.e.*, P2MP-TRXs on nodes and FS’ on fiber links, and we should try to minimize the total CAPEX due to them.

Fig. 2 shows an example on survivable WSON planning with SBPP. Here, we assume that two hub P2MP-TRXs are placed on *Node 2*, and their leaf P2MP-TRXs are deployed on *Nodes 1, 3 and 5*. Each traffic demand is denoted as $d_i(s, d, BW)$, where i is the index of its hub P2MP-TRX, s and d are its source and destination nodes, and BW represents its bandwidth requirement in SCs. Hence, the first hub P2MP-TRX is at 400 Gbps and only has one leaf P2MP-TRX on *Node 1*, while the second hub P2MP-TRX is at 100 Gbps and has two leaf P2MP-TRXs on *Nodes 3 and 5*, respectively. The solid and dashed lines in the figure indicates working and backup paths, respectively. We can see that as the working path of $d_1(2, 1, 4$ SCs) does not share any link with that of

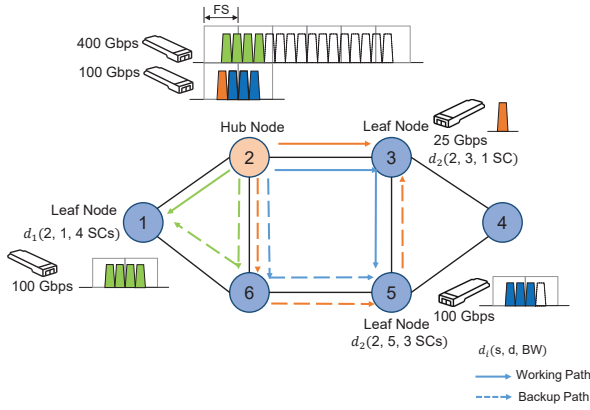


Fig. 2. Example on survivable WSON planning with SBPP.

$d_2(2, 3, 1 \text{ SC})$ or $d_2(2, 5, 3 \text{ SCs})$, and thus the backup path of $d_1(2, 1, 4 \text{ SCs})$ can share FS' with those of $d_2(2, 3, 1 \text{ SC})$ and $d_2(2, 5, 3 \text{ SCs})$ on the common link (*i.e.*, *Link* 2-6).

In order to quantify the protection efficiency of SBPP, we define the spectrum sharing ratio (SSR) as

$$\eta = 1 - \frac{F_b}{F'_b}, \quad (1)$$

where F_b and F'_b are the total numbers of backup FS' reserved with SBPP and with dedicated path protection (DPP), respectively. For the example in Fig. 2, SBPP should reserve sufficient FS' on the backup path of $d_1(2, 1, 4 \text{ SCs})$, *i.e.*, two FS' should be reserved on *Links* 2-6 and 6-1, respectively. As for $d_2(2, 3, 1 \text{ SC})$ or $d_2(2, 5, 3 \text{ SCs})$, their backup paths can share FS' with that of $d_1(2, 1, 4 \text{ SCs})$ since the working path of $d_1(2, 1, 4 \text{ SCs})$ does not share any link with that of $d_2(2, 3, 1 \text{ SC})$ or $d_2(2, 5, 3 \text{ SCs})$. Hence, there is no need to reserve additional FS' on *Link* 2-6. Then, two FS' need to be reserved on *Link* 6-5 for the backup paths of $d_2(2, 3, 1 \text{ SC})$ and $d_2(2, 5, 3 \text{ SCs})$, and an FS needs to be reserved on *Link* 5-3 for the backup path of $d_2(2, 3, 1 \text{ SC})$. To this end, the total number of backup FS' reserved for the demands with SBPP is $F_b = 2 \times 2 + 1 \times 2 + 1 \times 1 = 7$ (FS'·hops). When DPP is used, the only difference is that on *Link* 2-6, two additional FS' need to be reserved for the backup paths of $d_2(2, 3, 1 \text{ SC})$ and $d_2(2, 5, 3 \text{ SCs})$, and thus the total number of backup FS' reserved for the demands with DPP is $F'_b = F_b + 1 \times 2 = 9$ (FS'·hops). Therefore, the SSR is $\eta = 1 - \frac{7}{9} = \frac{2}{9}$.

IV. ILP MODEL

In this section, we formulate an ILP model to optimize the survivable planning of a WSON with P2MP-TRXs.

Parameters:

- $G(V, E)$: the topology of the WSON.
- $\mathbf{D} = [d_{h,l}]_{|H| \times |L|}$: the traffic matrix, where H and L denote the sets of hub and leaf nodes, respectively.
- ξ : the bandwidth of each SC.
- κ : the bandwidth of each FS.
- ω : the number of SCs that a link $e \in E$ can accommodate.
- Ω : the number of FS' that a link $e \in E$ can accommodate.

- \hat{T} : the maximum number of hub or leaf P2MP-TRXs that can be placed on each node $v \in V$ (*i.e.*, hub and leaf P2MP-TRXs are counted separately on each v).
- O_h/O_l : the set of the capacities of hub/leaf P2MP-TRXs.
- C_o : the cost of a type- o P2MP-TRX ($o \in O_h \cup O_l$).
- G_o/g_o : the maximum number of FS'/SCs that a type- o P2MP-TRX can occupy/use ($o \in O_h \cup O_l$), respectively.
- P : the set of pre-calculated routing paths.
- I_p : the integer indicator that equals 1 if the length of path p does not exceed 500 km, and 2 otherwise ($p \in P$).
- $B_{e,p}$: the boolean indicator that equals 1 if path p uses link e , and 0 otherwise ($p \in P, e \in E$).
- ϖ_o : the parameter introduced to facilitate the mapping between SCs and FS', which is the bandwidth difference between the FS' and SCs used by a type- o P2MP-TRX.

Decision Variables:

- $T_{h,m}^o$: the boolean variable that equals 1 if the m -th hub P2MP-TRX on node h is in type- o , and 0 otherwise.
- $M_{h,l}$: the indicator that equals 1 if hub-leaf P2MP-TRX pair $h-l$ can use SCs under DP-16QAM, and 2 otherwise.
- $\lambda_{l,p}^{h,m}$: the boolean variable that equals 1 if the leaf P2MP-TRX on node l uses p as the working path to talk with the m -th hub P2MP-TRX on node h , and 0 otherwise.
- $\phi_{l,p}^{h,m}$: the boolean variable that equals 1 if the leaf P2MP-TRX on node l reserves p as the backup path to talk with the m -th hub P2MP-TRX on node h , and 0 otherwise.
- $F_{h,m}$: the smallest start index of the FS' that can be used by the m -th hub P2MP-TRX on node h .
- $S_{h,m}^l/E_{h,m}^l$: the start/end index of the SCs that the m -th hub P2MP-TRX on node h allocates to leaf node l .
- $V_{h,m}^{l,n,o}$: the boolean variable that equals 1 if the m -th hub P2MP-TRX on node h talks with the n -th leaf P2MP-TRX on node l , which is in type- o , and 0 otherwise.

Intermediate Variables¹:

- \mathcal{F} : the maximum index of used FS' (MIFS) in the WSON.
- $t_{l,n}^o$: the boolean variable that equals 1 if the n -th leaf P2MP on node l is in type- o , and 0 otherwise.
- $\tilde{S}_{h,m}^l/\tilde{E}_{h,m}^l$: the start/end index of the FS' that the m -th hub P2MP-TRX on node h allocates to leaf node l .
- $\tau_{h,m}^{l_1,l_2}$: the boolean variable that equals 0 if SCs from the m -th hub P2MP-TRX on node h to leaf node l_1 use lower indices than those to leaf node l_2 (*i.e.*, $E_{h,m}^{l_1} < S_{h,m}^{l_2}$), and 1 otherwise.
- $\delta_{h_1,m_1,l_1}^{h_2,m_2,l_2}$: the boolean variable that equals 0 if FS' from the m_1 -th hub P2MP-TRX on h_1 to leaf node l_1 use lower indices than those from the m_2 -th hub P2MP-TRX on h_2 to leaf node l_2 (*i.e.*, $\tilde{E}_{h_1,m_1}^{l_1} < \tilde{S}_{h_2,m_2}^{l_2}$), and 1 otherwise.

Objective:

We design the optimization objective as to minimize the total CAPEX due to P2MP-TRX and FS usages

$$\text{Minimize } \alpha \cdot (C_{\text{hub}} + C_{\text{leaf}}) + \mathcal{F}, \quad (2)$$

where C_{hub} is the total cost of hub P2MP-TRXs as

$$C_{\text{hub}} = \sum_{h \in H} \sum_{m=1}^{\hat{T}} \sum_{o \in O_h} T_{h,m}^o \cdot C_o, \quad (3)$$

¹Here, we define the intermediate variables as those whose values can be calculated with the decision variables.

C_{leaf} is the total cost of leaf P2MP-TRXs as

$$C_{\text{leaf}} = \sum_{l \in L} \sum_{n=1}^{\hat{T}} \sum_{o \in O_l} t_{l,n}^o \cdot C_o, \quad (4)$$

and α is the adjustable weight for balancing the importance between P2MP-TRX usage and FS usage.

Constraints:

1) Constraints on P2MP-TRX Selection:

$$\sum_{o \in O_h} T_{h,m}^o \leq 1, \quad \forall h \in H, m \in [1, \hat{T}]. \quad (5)$$

Eq. (5) ensures that each deployed hub P2MP-TRX should only use one type of capacity.

$$\sum_{o \in O_l} t_{l,n}^o \leq 1, \quad \forall l \in L, n \in [1, \hat{T}]. \quad (6)$$

Eq. (6) ensures that each deployed leaf P2MP-TRX should only use one type of capacity.

2) Constraints on Lightpath Routing:

$$\sum_{p \in P} \lambda_{l,p}^{h,m} \leq 1, \quad \{l \in L, h \in H : l \neq h\}, \forall m \in [1, \hat{T}]. \quad (7)$$

Eq. (7) ensures that at most one working lightpath is set up between each pair of hub-leaf P2MP-TRXs.

$$\sum_{p \in P} \phi_{l,p}^{h,m} = \sum_{p \in P} \lambda_{l,p}^{h,m}, \quad \{l \in L, h \in H : l \neq h\}, \forall m \in [1, \hat{T}]. \quad (8)$$

Eq. (8) ensures that $\sum_{p \in P} \phi_{l,p}^{h,m}$ and $\sum_{p \in P} \lambda_{l,p}^{h,m}$ are always the same. Then, Eqs. (7)-(8) make sure that at most one backup lightpath is reserved for each pair of hub-leaf P2MP-TRXs.

$$\sum_{p \in P} \lambda_{l,p}^{h,m} \cdot B_{e,p} + \sum_{p \in P} \phi_{l,p}^{h,m} \cdot B_{e,p} \leq 1, \quad \{l \in L, h \in H : l \neq h\}, \forall m \in [1, \hat{T}], e \in E. \quad (9)$$

Eq. (9) ensures that the working and backup lightpaths for each pair of hub-leaf P2MP-TRXs have to be link-disjoint.

$$\begin{cases} \sum_{p \in P} \lambda_{l,p}^{h,m} \cdot I_p \leq M_{h,l}, \\ \sum_{p \in P} \phi_{l,p}^{h,m} \cdot I_p \leq M_{h,l}, \end{cases} \quad \{l \in L, h \in H : l \neq h\}, \forall m. \quad (10)$$

Eq. (10) ensures that the working and backup lightpaths allocated for each pair of hub-leaf P2MP-TRXs have to satisfy the QoT requirement of a same modulation format.

3) Constraints on Connections among P2MP-TRXs:

$$\sum_{\{h \in H : h \neq l\}} \sum_{m=1}^{\hat{T}} V_{h,m}^{l,n,o} = t_{l,n}^o, \quad \forall l \in L, n \in [1, \hat{T}], o \in O_l. \quad (11)$$

Eq. (11) ensures the relation between $V_{h,m}^{l,n,o}$ and $t_{l,n}^o$.

$$\sum_{o \in O_l} V_{h,m}^{l,n,o} \leq \sum_{p \in P} \lambda_{l,p}^{h,m}, \quad \{l \in L, h \in H : l \neq h\}, \forall m, n \in [1, \hat{T}], \quad (12)$$

$$\sum_{p \in P} \lambda_{l,p}^{h,m} \leq \sum_{n=1}^{\hat{T}} \sum_{o \in O_l} V_{h,m}^{l,n,o}, \quad \{l \in L, h \in H : l \neq h\}, \forall m. \quad (13)$$

Eqs. (12)-(13) ensure the relation between $V_{h,m}^{l,n,o}$ and $\lambda_{l,p}^{h,m}$.

4) Constraints on Capacities of P2MP-TRXs:

$$\sum_{\{l \in L : l \neq h\}} \left(E_{h,m}^l - S_{h,m}^l + 1 \right) \leq \sum_{o \in O_h} T_{h,m}^o \cdot g_o, \quad \forall h \in H, m. \quad (14)$$

Eq. (14) ensures that the SCs assigned to its leaf P2MP-TRXs do not exceed the capacity of the m -th hub P2MP-TRX at h .

$$d_{h,l} \cdot M_{h,l} \leq \sum_{m=1}^{\hat{T}} \left(E_{h,m}^l - S_{h,m}^l + 1 \right), \quad \{l \in L, h \in H : l \neq h\}. \quad (15)$$

Eq. (15) ensures that SCs allocated between each pair of hub-leaf P2MP-TRXs can satisfy the corresponding traffic demand.

$$E_{h,m}^l - S_{h,m}^l + 1 \leq \sum_{n=1}^{\hat{T}} \sum_{o \in O_l} V_{h,m}^{l,n,o} \cdot g_o, \quad \{l \in L, h \in H : l \neq h\}, \forall m. \quad (16)$$

Eq. (16) ensures that the capacity (in SCs) of each P2MP-TRX can accommodate the SCs assigned to it.

5) Constraints on Mapping between SCs and FS':

$$\tilde{S}_{h,m}^l = F_{h,m} + \frac{1}{\kappa} \left[\left(S_{h,m}^l - 1 \right) \cdot \xi + \sum_{o \in O_h} T_{h,m}^o \cdot \varpi_o \right], \quad \{l \in L, h \in H : l \neq h\}, \forall m. \quad (17)$$

Eq. (17) determines the mapping between $\tilde{S}_{h,m}^l$ and $S_{h,m}^l$.

$$\begin{aligned} \tilde{E}_{h,m}^l &= F_{h,m} - 1 + \sum_{o \in O_h} T_{h,m}^o \cdot g_o \\ &- \frac{1}{\kappa} \left[\left(\sum_{o \in O_h} T_{h,m}^o \cdot G_o - E_{h,m}^l \right) \cdot \xi + \sum_{o \in O_h} T_{h,m}^o \cdot \varpi_o \right], \end{aligned} \quad \{l \in L, h \in H : l \neq h\}, \forall m. \quad (18)$$

Eq. (18) determines the mapping between $\tilde{E}_{h,m}^l$ and $E_{h,m}^l$.

6) Constraints on SC and FS Assignments:

$$\begin{cases} \tau_{h,m}^{l_1,l_2} + \tau_{h,m}^{l_2,l_1} = 1, \\ E_{h,m}^{l_1} - S_{h,m}^{l_2} \leq \omega \cdot \left(\tau_{h,m}^{l_1,l_2} + 2 - \sum_{p \in P} \lambda_{l_1,p}^{h,m} - \sum_{p \in P} \lambda_{l_2,p}^{h,m} \right) - 1, \end{cases} \quad \{l_1, l_2 \in L, h \in H : l_1 \neq l_2, l_1 \neq h, l_2 \neq h\}, m \in [1, \hat{T}]. \quad (19)$$

Eq. (19) ensures that the SCs allocated from a same hub P2MP-TRX to two different leaf P2MP-TRXs do not overlap.

$$\begin{cases} \delta_{h_1,m_1,l_1}^{h_2,m_2,l_2} + \delta_{h_2,m_2,l_2}^{h_1,m_1,l_1} = 1, \\ \tilde{E}_{h_1,m_1}^{l_1} - \tilde{S}_{h_2,m_2}^{l_2} \leq \Omega \cdot \left(\delta_{h_1,m_1,l_1}^{h_2,m_2,l_2} + 4 - \sum_{p \in P} \lambda_{l_1,p}^{h_1,m_1} \cdot B_{e,p} \right. \\ \left. - \sum_{p \in P} \lambda_{l_2,p}^{h_2,m_2} \cdot B_{e,p} - \sum_{p \in P} \lambda_{l_1,p}^{h_1,m_1} - \sum_{p \in P} \lambda_{l_2,p}^{h_2,m_2} \right) - 1, \end{cases} \quad \{l_1, l_2 \in L, h_1, h_2 \in H : l_1 \neq h_1, l_2 \neq h_2\}, \\ \{m_1, m_2 \in [1, \hat{T}] : m_1 \neq m_2\}, \forall e \in E. \quad (20)$$

Eq. (20) ensures that the working lightpaths of two hub-leaf P2MP-TRX pairs (h_1 - l_1 and h_2 - l_2) should use non-overlapped

FS' if they share common link(s).

$$\left\{ \begin{array}{l} \delta_{h_1, m_1, l_1}^{h_2, m_2, l_2} + \delta_{h_2, m_2, l_2}^{h_1, m_1, l_1} = 1, \\ \tilde{E}_{h_1, m_1}^{l_1} - \tilde{S}_{h_2, m_2}^{l_2} \leq \Omega \cdot \left(\delta_{h_1, m_1, l_1}^{h_2, m_2, l_2} + 2 - \sum_{p \in P} \lambda_{l_1, p}^{h_1, m_1} \cdot B_{e, p} \right. \\ \left. - \sum_{p \in P} \phi_{l_2, p}^{h_2, m_2} \cdot B_{e, p} \right) - 1, \\ \tilde{E}_{h_1, m_1}^{l_1} - \tilde{S}_{h_2, m_2}^{l_2} \leq \Omega \cdot \left(\delta_{h_1, m_1, l_1}^{h_2, m_2, l_2} + 2 - \sum_{p \in P} \phi_{l_1, p}^{h_1, m_1} \cdot B_{e, p} \right. \\ \left. - \sum_{p \in P} \lambda_{l_2, p}^{h_2, m_2} \cdot B_{e, p} \right) - 1, \\ \{l_1, l_2 \in L, h_1, h_2 \in H : l_1 \neq h_1, l_2 \neq h_2\}, \\ \{m_1, m_2 \in [1, \hat{T}] : m_1 \neq m_2\}, \forall e \in E. \end{array} \right. \quad (21)$$

Eq. (21) indicates that the working and backup lightpaths of two hub-leaf P2MP-TRX pairs (h_1 - l_1 and h_2 - l_2), respectively, should use non-overlapped FS' if they share common link(s).

7) *Constraints on Variable Ranges:*

$$S_{h, m}^l \geq 1, \{l \in L, h \in H : l \neq h\}, \forall m. \quad (22)$$

Eq. (22) ensures that the start index of SCs used by any P2MP-TRX is not less than 1.

$$1 \leq F_{h, m} \leq \Omega - \sum_{o \in O_h} T_{h, m}^o \cdot G_o + 1, \forall h \in H, m \in [1, \hat{T}]. \quad (23)$$

Eq. (23) ensures that the smallest start index of the FS' used by each hub P2MP-TRX is set correctly.

$$\left\{ \begin{array}{l} F_{h, m} \leq \tilde{S}_{h, m}^l, \\ \tilde{S}_{h, m}^l \leq \Omega, \quad \{l \in L, h \in H : l \neq h\}, \forall m. \\ \tilde{E}_{h, m}^l \leq \Omega, \end{array} \right. \quad (24)$$

Eq. (24) ensures that the range of the FS' used by each hub P2MP-TRX is set correctly.

$$\tilde{E}_{h, m}^l \leq \mathcal{F}, \{l \in L, h \in H : l \neq h\}, \forall m. \quad (25)$$

Eq. (25) determines the MIFS \mathcal{F} in the planned WSON.

Complexity Analysis: The ILP model contains $|H| \cdot (\hat{T} \cdot (|L| \cdot (2|P| + 2 + \hat{T} \cdot |O_l|) + 1 + |O_h|) + |L|)$ decision variables, $|L| \cdot \hat{T} \cdot (|H| \cdot (2 + |L| + \hat{T} \cdot |H| \cdot |L|) + |O_l|)$ intermediate variables, and $(\hat{T} \cdot (|H| \cdot |L| \cdot (11 + |E| + \hat{T} + 2|L| + |H| \cdot |L| \cdot \hat{T} \cdot (2 + 3|E|)) + 4|H| + |L| \cdot (1 + |O_l|)) + |H| \cdot |L|)$ constraints.

V. HEURISTIC ALGORITHM DESIGN

Although the ILP in the previous section can obtain the optimal solution of the network planning, solving it can be time-consuming or even intractable, especially for large-scale problems. Therefore, in this section, we design a time-efficient heuristic to plan survivable WSONs with P2MP-TRXs quickly. Intuitively, the network planning can be solved with a greedy approach that handles the traffic demands in \mathbf{D} one by one. For each demand, we first calculate K shortest paths between its source and destination, and then for each of the paths, we get a link-disjoint shortest path. Hence, K pairs of link-disjoint paths can be obtained, among which we select an optimal one such that using the paths in it as the working and backup paths of the demand leads to the least FS usage.

Next, we allocate hub and leaf P2MP-TRXs according to the demand's bandwidth requirement, and use the first-fit scheme to assign SCs and FS'. We refer to this greedy algorithm as GRD-FF. Moreover, considering the fact that first-fit might not perform well for survivable EON planning [34, 43], we also design another greedy algorithm, namely, GRD-CF. The only difference from GRD-FF is that GRD-CF starts from the center of the spectrum on each fiber-link to assign FS' to lightpaths, *i.e.*, when searching for available FS', it moves towards both spectral ends to find the best FS block to assign to a lightpath. However, these two greedy algorithms might not achieve good spectrum sharing among backup lightpaths to improve the protection efficiency, and can lead to unnecessary P2MP-TRX and FS usages in the planned WSONs.

This motivates us to design a more effective heuristic based on adaptive demand grouping (ADG). Specifically, we try to groom traffic demands in groups before actually starting the network planning, such that the demands in each group can be served by a set of hub-leaf P2MP-TRXs. The purpose of the ADG is that for each hub node, we try to include its leaf nodes among which the distances are relatively short in the same group. By doing so, the demands in the same group can be routed in the way that uses as few links as possible, and thus effective spectrum saving can be achieved. Then, when setting up the working and backup lightpaths, we consider both the intra-group and inter-group information to increase the spectrum sharing among backup lightpaths. Based on these considerations, we design three sub-procedures for the ADG-based heuristic (namely, ADG): *Algorithm 1* for grouping the traffic demands in \mathbf{D} , and *Algorithm 2* for setting up lightpaths and assigning FS' to them based on the demand groups, which invokes *Algorithm 3* to route backup lightpaths for a specific group and assign FS' to its working and backup lightpaths.

A. Grouping Traffic Demands

Algorithm 1 shows the procedure for grouping demands. Here, we assume that all the lightpaths can use the high-level modulation format (*i.e.*, DP-16QAM), and then the required types and number of hub P2MP-TRXs can be estimated for each demand group. Next, in *Algorithm 2*, we determine the actual modulation format that can be used for each lightpath after its routing path has been selected. Specifically, if a lightpath can only use the low-level modulation format (*i.e.*, DP-QPSK), we will allocate more SCs to it and even assign new P2MP-TRXs to carry its bandwidth requirement if necessary.

The for-loop of *Lines 1-25* groups the demands on each hub node $h \in H$ to allocate hub P2MP-TRXs to h and assign demands to them. In each iteration, *Line 2* obtains the total capacity of the demands on h as Θ , and initializes $flag = 0$, which will be used in the while-loop covering *Lines 8-23*. Next, we select a set of hub P2MP-TRXs greedily to satisfy Θ , by first allocating a few hub P2MP-TRXs whose capacities are the largest to approach to Θ and then assigning those with smaller capacities to serve the remaining demands (*Line 3*).

The obtained hub P2MP-TRXs are then stored in set \mathbf{T}_h together with their capacities (*Line 4*). The for-loop of *Lines 5-7* checks each hub P2MP-TRX $T_i \in \mathbf{T}_h$, randomly assigns

Algorithm 1: Adaptive demand grouping

Input: Topology of WSON $G(V, E)$, traffic demands \mathbf{D} .
Output: Demand groups \mathbb{G} .

```

1 for each hub node  $h \in H$  do
2    $\Theta = \sum_{\{l \in L: l \neq h\}} d_{h,l}$ ,  $flag = 0$ ,  $j = 0$ ;
3   select a set of hub P2MP-TRXs greedily (largest
   capacity first) to satisfy  $\Theta$ ;
4   store the hub P2MP-TRXs in set  $\mathbf{T}_h$ ;
5   for each hub P2MP-TRX  $T_i \in \mathbf{T}_h$  do
6     randomly select a demand  $d_{h,l}$  to assign to  $T_i$ 
     and mark node  $l$  as its center leaf  $L_i$ ;
7   end
8   while  $flag = 0$  OR  $j < M$  do
9      $flag = 1$ ,  $j = j + 1$ ;
10    for each hub P2MP-TRX  $T_i \in \mathbf{T}_h$  do
11      remove all the demands assigned to  $T_i$  except
      for the one to its center leaf  $L_i$ ;
12    end
13    for each unassigned demand  $d_{h,l}$  do
14      find the hub P2MP-TRX  $T_i \in \mathbf{T}_h$  that can
      carry  $d_{h,l}$  and provide the smallest  $\rho(l, L_i)$ ;
15      assign  $d_{h,l}$  to  $T_i$  and update its capacity;
16    end
17    for each hub P2MP-TRX  $T_i \in \mathbf{T}_h$  do
18      recalculate its center leaf  $L_i$  with Eq. (26);
19      if  $L_i$  has been changed then
20         $flag = 0$ ;
21      end
22    end
23  end
24  store  $\mathbf{T}_h$  and the demands assigned to each hub
  P2MP-TRX in it in  $\mathbb{G}$ ;
25 end
26 return  $\mathbb{G}$ ;

```

a demand $d_{h,l}$ to it, and marks the leaf node l of $d_{h,l}$ as the center leaf of T_i (i.e., $L_i = l$). Next, the while-loop of Lines 8-23 optimizes the demands assigned to each hub P2MP-TRX $T_i \in \mathbf{T}_h$ until no further optimization can be made or reach the maximum iterations. Here, Line 9 sets $flag = 1$ and Lines 10-12 re-initialize the demand assigned to each hub P2MP-TRX $T_i \in \mathbf{T}_h$. Then, we check each unassigned demand $d_{h,l}$ and assign it to the hub P2MP-TRX that still has enough remaining capacity to carry it and provides the smallest $\rho(l, L_i)$ (Lines 13-16), where $\rho(u, v)$ is the function to get the length of the shortest path between nodes u and v . Although all the hub P2MP-TRXs $\{T_i \in \mathbf{T}_h\}$ are on hub node h , their center leaves $\{L_i\}$ can be on different nodes, i.e., $\rho(l, L_i)$ can be different when i changes. Hence, we leveraging the one-to-one mapping between L_i and T_i to select a hub P2MP-TRX for the demand $d_{h,l}$. Specifically, as shown in Lines 14-15, we choose the hub P2MP-TRX $T_i \in \mathbf{T}_h$ with the smallest $\rho(l, L_i)$ to carry $d_{h,l}$.

At this point, we have grouped the demands on hub node h once, but the grouping scheme might not be optimal yet. Hence, we will optimize the grouping scheme in M iterations

at most. Specifically, in each new iteration, we first recalculate the center leaf L_i of each hub P2MP-TRX $T_i \in \mathbf{T}_h$ (Lines 17-22), i.e., for the demands assigned to T_i (denoted with set \mathbf{D}_i), the center leaf is recalculated as

$$L_i = \operatorname{argmin}_{d_{h,l} \in \mathbf{D}_i} \left(\sum_{\{d_{h,l'} \in \mathbf{D}_i: l' \neq l\}} \rho(l', l) \right). \quad (26)$$

If the recalculated center leaf is different from the original one, we set $flag = 0$ (i.e., further optimization is still possible) (Lines 19-21). After all the demands on hub node h have been assigned to hub P2MP-TRXs, Line 24 stores the results in \mathbb{G} , where each hub P2MP-TRX corresponds to a demand group. Note that, for each hub P2MP-TRX $T_i \in \mathbf{T}_h$ on hub node h , the demand grouping in Algorithm 1 actually makes its leaf nodes as close to each other as possible. This is beneficial to the subsequent RSA of lightpaths in two manners: 1) the lightpaths of demands in a same group use as few links as possible, and 2) the high-level modulation format can be used to the maximum extent for saving spectrum resources.

B. Routing and Spectrum Assignment of Lightpaths

Algorithm 2 shows the procedure of setting up lightpaths (both working and backup ones) and assigning FS' based on the grouping results in \mathbb{G} . Here, to avoid spectrum fragmentation and maximize FS usage on fiber links, we leverage the layered auxiliary graph (LAG) based approach [44] to get the RSA schemes of lightpaths. The LAG-based approach was proposed for integrated multicast-capable RSA, and thus can be used to tackle the RSA related to P2MP-TRXs. Specifically, for each demand group that will be provisioned with a hub P2MP-TRX and its leaf P2MP-TRXs, we first decompose the WSON topology into several LAGs according to the FS usages in the WSON, and then based on the capacities of the demands in the group, we select a proper LAG and calculate the demands' working and backup lightpaths in it. Note that, Algorithm 3 is a sub-procedure of Algorithm 2 and will be called to route backup lightpaths for a specific group and assign FS' to its working and backup lightpaths.

In Algorithm 2, Lines 1-2 are for the initialization, where for each group $T_i \in \mathbb{G}$, we first put the demands in D_h^i and the type of T_i in C_h^i , and then sort $\{D_h^i\}$ in descending order of capacity. The type of T_i is just the capacity of its hub P2MP-TRX (in the number of FS' by assuming that DP-16QAM is used). For example, if the capacity of T_i is 400 Gbps, its hub P2MP-TRX will output 16 SCs with a total spectrum usage of 64 GHz, which can only be accommodated with at least 6 FS' ($C_h^i = 6$). The for-loop of Lines 3-24 obtains the RSA schemes for the lightpaths of each group. Here, k denotes the start FS of the current LAG, and as the number of available FS on each fiber link is F , k varies from 1 to $F - C_h^i + 1$ for D_h^i . The for-loop of Lines 4-23 is to find the RSA schemes for the lightpaths of D_h^i in the k -th LAG. We use $flag$ to indicate whether the current LAG is available for carrying the lightpaths of each demand in D_h^i , which is initialized as 0 in Line 5. If the current LAG is unavailable, we set $flag = 1$ and proceed to the next LAG, i.e., the $(k + 1)$ -th LAG.

Specifically, *Lines* 5-10 explain how to build the k -th LAG $G^k(V^k, E^k)$ according to the FS usages in the WSON and the total capacity of demands in D_h^i (in FS'). The for-loop of *Lines* 11-16 calculates a working lightpath for each demand $d_{h,l} \in D_h^i$ in the k -th LAG. If the lightpath cannot be obtained, we set the $flag = 1$ and proceed to the next LAG (*Lines* 13-15). If the working lightpaths of all the demands in D_h^i can be found, we invoke *Algorithm 3* to route their backup lightpaths and assign FS' to all the lightpaths (*Line* 18). Then, if *Algorithm 3* returns $flag = 0$, the RSA schemes of the working and backup lightpaths of all the demands in D_h^i have been determined in the current LAG, and thus the for-loop of *Lines* 3-24 can be exited (*Lines* 19-21). Finally, the for-loop of *Lines* 25-30 checks the working and backup lightpaths of each demand to see whether their lengths satisfy the QoT requirement of DP-16QAM (the high-level modulation format). If not, *Line* 27 downgrades the modulation format to DP-QPSK and serves the remaining capacity first with deployed P2MP-TRXs that still have spare capacities and then with a new P2MP-TRX.

In *Algorithm 3*, *Line* 1 is for the initialization, where E^k is the set to store available links for backup lightpaths and $flag$ here is the indicator to tell whether the backup lightpath of demand $d_{h,l} \in D_h^i$ has been found. The for-loop of *Lines* 2-6 checks each link $e \in E$, and if the FS block $[k, (k+C_h^i-1)]$ on e is either available or only used by other backup lightpaths, we insert e into E^k as e^k . The for-loop covering *Lines* 7-18 determines the backup lightpath for each demand in D_h^i . *Line* 8 first sets $E_l = E^k$, where E_l is a temporary link set for calculating the backup lightpath of $d_{h,l}$ in subsequent steps, then removes the links on the working lightpath p_w^l from E_l and calculates weight W_e^k of each link $e \in E_l$ as

$$W_e^k = \sum_{i=k}^{k+C_h^i-1} b_e^i, \quad (27)$$

where b_e^i indicates the state of the i -th FS on link e , *i.e.*, we have $b_e^i = 0$ if the i -th FS on link e is used by other backup lightpaths, and $b_e^i = 1$ otherwise. Apparently, W_e^k becomes smaller if more FS' in the FS block $[k, k+C_h^i-1]$ have been used by other backup lightpaths, which means that if we use e on the current demand's backup lightpath, the opportunity of spectrum sharing among backup lightpaths becomes larger.

Line 9 gets K shortest paths between h and l in $G^k(V^k, E_l)$ according to weight $\{W_e^k\}$, and put them and their weights in sets P_p^l and \mathcal{W}^l , respectively². *Line* 10 checks whether set P_p^l can be obtained. If not, we know that the backup lightpath of $d_{h,l}$ cannot be found in the k -th LAG, and thus we set $flag = 1$ and $\{p_p^l\} = \emptyset$ (*Line* 11). As we have explained above, the less a path's weight is under weights $\{W_e^k\}$, the larger opportunity of spectrum sharing will be. However, the weights $\{W_e^k\}$ are calculated under the assumption that all the lightpaths can be provisioned with DP-16QAM. Therefore, *Line* 13 checks whether DP-16QAM can be used on a backup lightpath, and *Line* 14 doubles the weight of the backup

²Note that, the two-step routing calculation in *Lines* 8-9 can lose some valid solutions when the original topology $G(V, E)$ has relatively low connectivity. In our future work, we will address this issue by pre-calculating a set of link-disjoint paths between each node-pair in $G(V, E)$ (*i.e.*, the one-step approach).

Algorithm 2: Solving RSA of lightpaths with LAGs

Input: Topology of WSON $G(V, E)$, set of demand groups \mathbb{G} , and the number of FS' on each link F .

- 1 put demands assigned to T_i in D_h^i , and put the capacity of T_i in C_h^i ($T_i \in \mathbf{T}_h$, $h \in H$);
- 2 sort $\{D_h^i, h \in H\}$ in descending order of capacity;
- 3 **for each** D_h^i **in sorted order do**
- 4 **for** $k \in [1, F - C_h^i + 1]$ **do**
- 5 $flag = 0$, put each $v \in V$ in $G^k(V^k, E^k)$ as v^k ;
- 6 **for each link** $e \in E$ **do**
- 7 **if** FS block $[k, k + C_h^i - 1]$ **unused on** e **then**
- 8 insert e in $G^k(V^k, E^k)$ as e^k ;
- 9 **end**
- 10 **end**
- 11 **for each** $d_{h,l} \in D_h^i$ **with descending capacity do**
- 12 get the shortest path between h and l in $G^k(V^k, E^k)$ as p_w^l ;
- 13 **if** p_w^l **cannot be obtained then**
- 14 $flag = 1$, **break**;
- 15 **end**
- 16 **end**
- 17 **if** $flag = 0$ **then**
- 18 run *Algorithm 3*;
- 19 **if** $flag = 0$ **then**
- 20 mark $\{p_w^l\}$ and $\{p_p^l\}$ as working and backup paths of $d_{h,l} \in D_h^i$, **break**;
- 21 **end**
- 22 **end**
- 23 **end**
- 24 **end**
- 25 **for each demands** $d_{h,l} \in D_h^i$ ($h \in H$) **do**
- 26 **if** p_w^l or p_p^l **cannot use DP-16QAM then**
- 27 serve remaining capacity using deployed P2MP-TRXs with spare capacity or a new one;
- 28 update FS usages;
- 29 **end**
- 30 **end**

lightpath if not. Next, in *Line* 16, we select the path in P_p^l whose weight in \mathcal{W}^l is the smallest as the backup lightpath p_p^l of $d_{h,l}$. Finally, if we can find the backup lightpaths for all the demands in D_h^i in the k -th LAG, the for-loop of *Lines* 20-22 assigns FS' to both working and backup lightpaths of the demands, and updates the FS usages.

C. Complexity Analysis

The complexity of the for-loop of *Lines* 1-25 in *Algorithm 1* is $O(|V|^3 \cdot \mathcal{D}^2 \cdot \hat{g}^2)$, where $\mathcal{D} = \sum_{d_{h,l} \in \mathbf{D}} d_{h,l}$, and \hat{g} denotes the maximum number of SCs that any type of P2MP-TRX in $O_h \cup O_l$ can use. Hence, the time complexity of *Algorithm 1* is $O(|V|^3 \cdot \mathcal{D}^2 \cdot \hat{g}^2)$. As *Algorithm 3* is called in *Algorithm 2*, we first discuss its time complexity. The complexity of the for-loop of *Lines* 2-6 is $O(|E|)$, that of the for-loop of *Lines* 7-18 is $O(\hat{g} \cdot K \cdot |V| \cdot (|E| + |V| \cdot \log_2(|V|)))$, and the for-loop of *Lines* 20-22 runs for \hat{g} times at most. Therefore, the time complexity

Algorithm 3: Routing backup lightpaths and assigning FS'

Input: Current LAG $G^k(V^k, E^k)$, D_h^i , C_h^i , and $\{p_w^l\}$.
Output: $flag$, $\{p_p^l\}$, and FS usages on links.

- 1 $E^k = \emptyset$, $flag = 0$;
- 2 **for** each link $e \in E$ **do**
- 3 **if** FS block $[k, (k + C_h^i - 1)]$ on e is either available
 or only used by other backup lightpaths **then**
- 4 insert e in $G^k(V^k, E^k)$ as e^k ;
- 5 **end**
- 6 **end**
- 7 **for** each $d_{h,l} \in D_h^i$ with descending capacity **do**
- 8 $E_l = E^k$, remove links on p_w^l from E_l and calculate
 $\{W_e^k, e \in E_l\}$ with Eq. (27);
- 9 get K shortest paths between h and l in $G^k(V^k, E_l)$
 based on $\{W_e^k\}$ to put in set P_p^l (their weights in
 \mathcal{W}^l);
- 10 **if** P_p^l cannot be obtained **then**
- 11 $flag = 1$, $\{p_p^l\} = \emptyset$, **break**;
- 12 **else**
- 13 **if** i -th path in P_p^l can only use DP-QPSK **then**
- 14 double weight of the i -th path in \mathcal{W}^l ;
- 15 **end**
- 16 select the path in P_p^l whose weight in \mathcal{W}^l is the
 smallest as p_p^l ;
- 17 **end**
- 18 **end**
- 19 **if** $flag = 0$ **then**
- 20 **for** each $d_{h,l} \in D_h^i$ with descending capacity **do**
- 21 assign FS' within $[k, k + C_h^i - 1]$ for $d_{h,l}$, and
 update FS usages;
- 22 **end**
- 23 **end**
- 24 **return** $flag$, $\{p_p^l\}$, and FS usages on links;

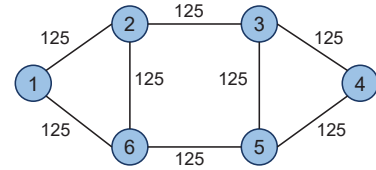
of Algorithm 3 is $O(\hat{g} \cdot K \cdot |V| \cdot (|E| + |V| \cdot \log_2(|V|)))$. The time complexity of Algorithm 2 can be analyzed as follows. The complexity of sorting in Line 2 is $O(\mathcal{D} \cdot \log_2(\mathcal{D}))$, the complexity of the for-loop of Lines 3-24 is $O(\mathcal{D} \cdot \hat{g} \cdot (\log_2(\hat{g}) + K \cdot |V| \cdot (|E| + |V| \cdot \log_2(|V|))))$ (including the time complexity of Algorithm 3), and the for-loop of Lines 25-30 runs for $\mathcal{D} \cdot \hat{g}$ times at most. Hence, the time complexity of Algorithm 2 is $O(\mathcal{D} \cdot (\hat{g} \cdot \log_2(\hat{g}) + \hat{g} \cdot K \cdot |V| \cdot (|E| + |V| \cdot \log_2(|V|)) + \log_2(\mathcal{D})))$. As ADG runs Algorithms 1 and 2 in sequence, its time complexity is the sum of those of the two algorithms.

VI. PERFORMANCE EVALUATIONS

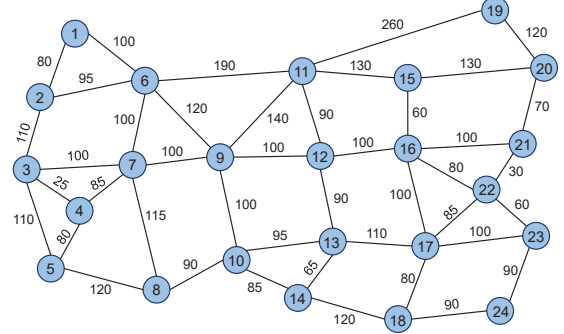
In this section, we discuss the numerical simulations for evaluating the performance of our proposed algorithms.

A. Simulation Setup

Our simulations consider two physical topologies for WSONs: 1) the 6-node topology in Fig. 3(a), and 2) the 24-node US Backbone topology (USB) in Fig. 3(b). We assume that each FS occupies a bandwidth of 12.5 GHz, and each fiber link can accommodate 358 FS' at most [5]. Meanwhile, according



(a) 6-node topology



(b) 24-node US Backbone topology

Fig. 3. Topologies of WSONs with link lengths in kilometers.

to the realistic settings in [13], we set the number of SCs that a 25/100/400-Gbps P2MP-TRX is 1/4/16, respectively, where each SC occupies 4 GHz. The actual capacity of each SC depends on the modulation format that it uses. In this work, we consider two modulation formats, *i.e.*, DP-16QAM and DP-QPSK, and the capacities that they can deliver with an SC are 25 and 12.5 Gbps, respectively. According to the discussions in [15], we assume that DP-16QAM can be used if the length of a lightpath does not exceed 500 km, whereas DP-QPSK has to be used for longer lightpaths. The capacity of a hub P2MP-TRX can be 100 or 400 Gbps, and that of a leaf P2MP-TRX can be 25 or 100 Gbps. A 25/100/400-Gbps P2MP-TRX can use 1/2/6 FS' at most, respectively. As for the costs of P2MP-TRXs, the ratio among the unit costs of 25/100/400-Gbps P2MP-TRXs is set as 1 : 2 : 4 [20].

Due to the time complexity of the ILP, it can only be solved for small-scale problems that use the 6-node topology. In the following discussion, we refer to the ADG-based heuristic designed in Section V (*i.e.*, the one that combines Algorithms 1-3) as ADG. In addition to ILP and ADG, we also consider the two greedy heuristics (GRD-CF and GRD-FF) mentioned at the beginning of Section V. As for the K shortest-path routing used in the algorithms, we set $K = 4$. The simulations evaluate the algorithms with three metrics: 1) the total CAPEX defined in Eq. (2), 2) the maximum index of used FS' (MIFS) in the WSON, and 3) the spectrum sharing ratio (SSR) defined in Eq. (1). To ensure statistical accuracy, we obtain each data point by averaging the results from 10 independent runs. The simulations run on a computer with 40 Intel(R) Xeon(R) Silver 4210 CPU @ 2.20 GHz and 64 GB memory, and the software environment is MATLAB 2022b with Gurobi 9.5.2 [45].

B. Small-Scale Simulations

We first conduct small-scale simulations with the 6-node topology to compare ILP, ADG, GRD-CF and GRD-FF. The maximum running time of ILP is set as 24 hours (86,400

seconds), and if an optimal solution cannot be obtained within the period, we just select the current best solution. In each simulation, we randomly generate H&S traffic demands in \mathbf{D} and make the range of total traffic within [1000, 2000] Gbps.

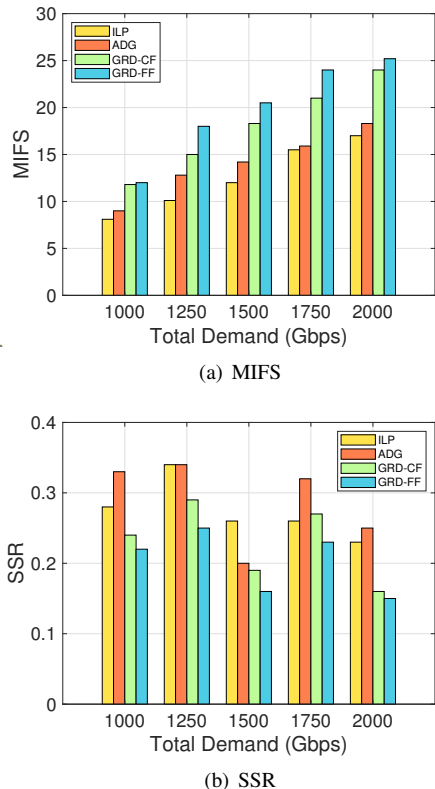


Fig. 4. Results of ILP, ADG, GRD-CF and GRD-FF with 6-node topology.

Table I summarizes the performance of the algorithms in this case. We can see that ILP always provides the smallest total CAPEX, followed by ADG, then GRD-CF, while GRD-FF always performs the worst. As for the running time, ILP is the most time-consuming one and its running time reaches the upper-limit all the time. Both GRD-CF and GRD-FF run faster than ADG, but the relative ratios between their running time decrease with the total traffic volume.

Fig. 4 further analyzes the algorithms' performance in MIFS and SSR. In Fig. 4(a), we can see that ADG approximates the optimal results from ILP better than GRD-CF and GRD-FF, and the spectrum saving achieved by ADG over GRD-CF and GRD-FF increases with the total traffic volume and is significant for the cases of 1,750 and 2,000 Gbps. Fig. 4(b) plots the results on SSR, which indicates that ADG provides a larger SSR than the two benchmarks in most cases, and for certain cases, the SSR from ADG can even be larger than that from ILP. This is because ADG pays special attention on increasing the sharing of backup spectrum resources.

C. Large-Scale Simulations

Next, we consider the USB topology for large-scale simulations and set the total traffic volume in \mathbf{D} within [5, 25] Tbps. This time, ILP becomes intractable and thus we only simulate

ADG, GRD-CF and GRD-FF. Fig. 5 compares the performance of the three algorithms, which verifies that ADG still outperforms GRD-CF and GRD-FF in terms of all the three metrics. With LAG, ADG optimizes the RSA of lightpaths better, achieving significant saving on FS usage. Specifically, related to GRD-CF and GRD-FF, ADG reduces MIFS by 42.05% and 46.52% on average, respectively. Table II lists the running time of the algorithms. As expected, ADG is the most time-consuming one among the algorithms and GRD-FF takes the shortest time for the network planning. Note that, even in the worst-case scenario, the running time of all the algorithms is still in seconds, which is short enough to be acceptable for solving network planning problems. Specifically, this work tackles the survivable network planning of a WSON based on P2MP-TRXs, which should be done by the operator before the WSON is actually built, and thus running time in minutes or even hours is common and acceptable. In all, the results in Fig. 5 and Table II confirm the effectiveness of our proposal.

Finally, we would like to comment on the scalability of ADG in terms of two key parameters, *i.e.*, the number of nodes in the topology $|V|$ and the number of candidate paths K . The time complexity analysis in Section V-C indicates that the running time of ADG will scale with $|V|$ in $O(|V|^3)$. The number of nodes in the USB topology is $|V| = 24$ with which the running time of ADG in the worst-case scenario is 7.108 seconds. Therefore, we can estimate that the running time of ADG with a 100-node topology (a fairly large one for metro-aggregation networks) will be in minutes, which is still acceptable for solving a network planning problem. The running time of ADG scales linearly with K . In general, a larger K provides more path candidates to ADG for the network planning, which would be beneficial. However, the number of shortest paths that can be found in a topology is limited by its connectivity, and thus the positive effect of increasing K on ADG will converge at certain point.

VII. CONCLUSION

This paper studied how to plan survivable WSONs with P2MP-TRXs and SBPP to address single-link failures. We first formulated an ILP model to place P2MP-TRXs, assign SCs to P2MP-TRXs, and calculate RSA for the working/backup light-path between each hub-leaf P2MP-TRX pair, such that a set of traffic demands can be satisfied with the minimum CAPEX. Then, a time-efficient heuristic based on ADG was proposed to solve the problem time-efficiently. Extensive simulations confirmed the performance of our ADG-based heuristic, *i.e.*, it can approximate the optimal results from the ILP well and outperform two greedy-based benchmarks significantly.

ACKNOWLEDGMENTS

This work was supported by NSFC project 61871357 and Fundamental Fund for Central Universities (WK3500000006).

REFERENCES

- [1] Z. Pan *et al.*, "Advanced optical-label routing system supporting multicast, optical TTL, and multimedia applications," *J. Lightw. Technol.*, vol. 23, pp. 3270–3281, Oct. 2005.

TABLE I
SIMULATION RESULTS WITH 6-NODE TOPOLOGY

Total Traffic Volume in D (Gbps)	ILP		ADG		GRD-CF		GRD-FF	
	Total CAPEX	Running Time (sec)						
1,000	14.90	86,400	15.44	0.0268	18.22	0.011	18.42	0.010
1,250	18.84	86,400	21.46	0.025	23.42	0.013	26.42	0.010
1,500	21.90	86,400	23.97	0.028	28.60	0.015	30.57	0.014
1,750	27.35	86,400	27.60	0.033	32.76	0.022	35.76	0.019
2,000	29.80	86,400	30.36	0.045	36.36	0.029	37.26	0.027

TABLE II
SIMULATION RESULTS WITH USB TOPOLOGY

Total Traffic Volume in D (Tbps)	ADG		GRD-CF		GRD-FF	
	Total CAPEX	Running Time (sec)	Total CAPEX	Running Time (sec)	Total CAPEX	Running Time (sec)
5	63.82	0.799	82.80	0.264	85.30	0.234
10	115.30	2.076	155.14	0.524	162.64	0.391
15	169.96	3.600	224.28	0.715	235.38	0.601
20	222.90	4.970	291.86	1.076	307.26	0.833
25	282.31	7.108	361.74	1.380	384.54	1.096

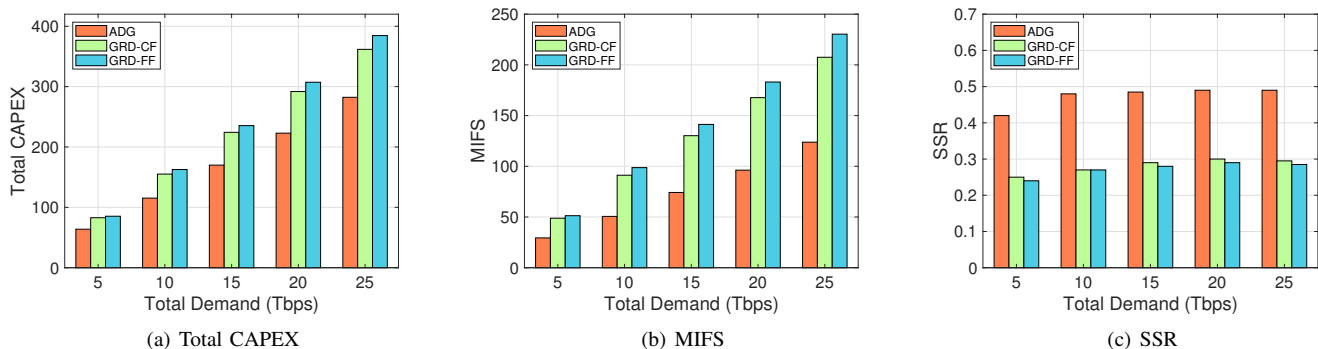


Fig. 5. Results of ADG, GRD-CF and GRD-FF with USB topology.

- [2] P. Lu *et al.*, "Highly-efficient data migration and backup for Big Data applications in elastic optical inter-datacenter networks," *IEEE Netw.*, vol. 29, pp. 36–42, Sept./Oct. 2015.
- [3] K. Wu, P. Lu, and Z. Zhu, "Distributed online scheduling and routing of multicast-oriented tasks for profit-driven cloud computing," *IEEE Commun. Lett.*, vol. 20, pp. 684–687, Apr. 2016.
- [4] V. Dukic *et al.*, "Beyond the mega-data center: networking multi-data center regions," in *Proc. of ACM SIGCOMM 2020*, pp. 765–781, Aug. 2020.
- [5] Z. Zhu, W. Lu, L. Zhang, and N. Ansari, "Dynamic service provisioning in elastic optical networks with hybrid single-/multi-path routing," *J. Lightw. Technol.*, vol. 31, pp. 15–22, Jan. 2013.
- [6] L. Gong *et al.*, "Efficient resource allocation for all-optical multicasting over spectrum-sliced elastic optical networks," *J. Opt. Commun. Netw.*, vol. 5, pp. 836–847, Aug. 2013.
- [7] W. Shi, Z. Zhu, M. Zhang, and N. Ansari, "On the effect of bandwidth fragmentation on blocking probability in elastic optical networks," *IEEE Trans. Commun.*, vol. 61, pp. 2970–2978, Jul. 2013.
- [8] Y. Yin *et al.*, "Spectral and spatial 2D fragmentation-aware routing and spectrum assignment algorithms in elastic optical networks," *J. Opt. Commun. Netw.*, vol. 5, pp. A100–A106, Oct. 2013.
- [9] C. Chen *et al.*, "Demonstrations of efficient online spectrum defragmentation in software-defined elastic optical networks," *J. Lightw. Technol.*, vol. 32, pp. 4701–4711, Dec. 2014.
- [10] M. Faruk *et al.*, "Coherent passive optical networks: Why, when, and how," *IEEE Commun. Mag.*, vol. 59, pp. 112–117, Dec. 2021.
- [11] A. Funnell, D. Butler, and G. Zervas, "Reconfigurable optical star network architecture for multicast media production data centres," *Opt. Switch. Netw.*, vol. 36, p. 100556, Feb. 2020.
- [12] J. Back *et al.*, "A filterless design with point-to-multipoint transceivers for cost-effective and challenging metro/regional aggregation topologies," in *Proc. of ONDM 2022*, pp. 1–6, May 2022.
- [13] D. Welch *et al.*, "Point-to-multipoint optical networks using coherent digital subcarriers," *J. Lightw. Technol.*, vol. 39, pp. 5232–5247, Aug. 2021.
- [14] M. Jinno *et al.*, "Multiflow optical transponder for efficient multilayer optical networking," *IEEE Commun. Mag.*, vol. 50, pp. 56–65, May 2012.
- [15] M. Hosseini *et al.*, "Long-term cost-effectiveness of metro networks exploiting point-to-multipoint transceivers," in *Proc. of ONDM 2022*, pp. 1–6, May 2022.
- [16] A. Rashidinejad *et al.*, "Real-time demonstration of 2.4Tbps (200Gbps/λ) bidirectional coherent DWDM-PON enabled by coherent Nyquist subcarriers," in *Proc. of OFC 2020*, pp. 1–3, Mar. 2020.
- [17] J. Back *et al.*, "CAPEX savings enabled by point-to-multipoint coherent pluggable optics using digital subcarrier multiplexing in metro aggregation networks," in *Proc. of ECOC 2020*, pp. 1–4, Dec. 2020.
- [18] N. Skorin-Kapov, F. Muro, M. Delgado, and P. Pavon-Marino, "Point-to-multipoint coherent optics for re-thinking the optical transport: Case study in 5G optical metro networks," in *Proc. of ONDM 2021*, pp. 1–4, Jun. 2021.
- [19] P. Pavon-Marino *et al.*, "On the benefits of point-to-multipoint coherent optics for multilayer capacity planning in ring networks with varying traffic profiles," *J. Opt. Commun. Netw.*, vol. 14, no. 5, pp. B30–B44,

May 2022.

- [20] M. Hosseini *et al.*, “Optimization of survivable filterless optical networks exploiting digital subcarrier multiplexing,” *J. Opt. Commun. Netw.*, vol. 14, pp. 586–594, Jul. 2022.
- [21] C. Tremblay *et al.*, “Filterless optical networks: a unique and novel passive WAN network solution,” in *Proc. of OECC/IOOC 2007*, pp. 466–467, Jul. 2007.
- [22] O. Ayoub *et al.*, “Tutorial on filterless optical networks,” *J. Opt. Commun. Netw.*, vol. 14, pp. 1–15, Mar. 2022.
- [23] Z. Zhu *et al.*, “RF photonics signal processing in subcarrier multiplexed optical-label switching communication systems,” *J. Lightw. Technol.*, vol. 21, pp. 3155–3166, Dec. 2003.
- [24] Y. Zhang, M. O’Sullivan, and R. Hui, “Digital subcarrier multiplexing for flexible spectral allocation in optical transport network,” *Opt. Express*, vol. 19, pp. 21 880–21 889, Oct. 2011.
- [25] “Finisar Single Wavelength Selective Switch (WSS).” [Online]. Available: https://finisarwss.com/wp-content/uploads/2020/07/FinisarWSS_Single_Wavelength_Selective_Switch_ProductBrief_Jun2020.pdf
- [26] Z. Zhu *et al.*, “Energy-efficient translucent optical transport networks with mixed regenerator placement,” *J. Lightw. Technol.*, vol. 30, pp. 3147–3156, Oct. 2012.
- [27] R. Govindan *et al.*, “Evolve or die: High-availability design principles drawn from Google’s network infrastructure,” in *Proc. of ACM SIGCOMM 2016*, pp. 58–72, Aug. 2016.
- [28] S. Tang *et al.*, “Sel-INT: A runtime-programmable selective in-band network telemetry system,” *IEEE Trans. Netw. Serv. Manag.*, vol. 17, pp. 708–721, Jun. 2020.
- [29] L. Gong and Z. Zhu, “Virtual optical network embedding (VONE) over elastic optical networks,” *J. Lightw. Technol.*, vol. 32, pp. 450–460, Feb. 2014.
- [30] J. Liu *et al.*, “On dynamic service function chain deployment and readjustment,” *IEEE Trans. Netw. Serv. Manag.*, vol. 14, pp. 543–553, Sept. 2017.
- [31] L. Gong, Y. Wen, Z. Zhu, and T. Lee, “Toward profit-seeking virtual network embedding algorithm via global resource capacity,” in *Proc. of INFOCOM 2014*, pp. 1–9, Apr. 2014.
- [32] J. Yin *et al.*, “Experimental demonstration of building and operating QoS-aware survivable vSD-EONs with transparent resiliency,” *Opt. Express*, vol. 25, pp. 15 468–15 480, 2017.
- [33] X. Chen, S. Zhu, L. Jiang, and Z. Zhu, “On spectrum efficient failure-independent path protection p-cycle design in elastic optical networks,” *J. Lightw. Technol.*, vol. 33, pp. 3719–3729, Sept. 2015.
- [34] F. Ji *et al.*, “Dynamic p-cycle protection in spectrum-sliced elastic optical networks,” *J. Lightw. Technol.*, vol. 32, pp. 1190–1199, Mar. 2014.
- [35] Z. Zhu *et al.*, “Demonstration of cooperative resource allocation in an OpenFlow-controlled multidomain and multinational SD-EON testbed,” *J. Lightw. Technol.*, vol. 33, pp. 1508–1514, Apr. 2015.
- [36] S. Li *et al.*, “Protocol oblivious forwarding (POF): Software-defined networking with enhanced programmability,” *IEEE Netw.*, vol. 31, pp. 58–66, Mar./Apr. 2017.
- [37] X. Chen *et al.*, “Flexible availability-aware differentiated protection in software-defined elastic optical networks,” *J. Lightw. Technol.*, vol. 33, pp. 3872–3882, Sept. 2015.
- [38] “The ultimate guide to Nyquist subcarriers.” [Online]. Available: <https://www.infinera.com/wp-content/uploads/The-Ultimate-Guide-to-Nyquist-Subcarriers-0208-WP-RevA-0719.pdf>.
- [39] A. Napoli *et al.*, “Live network demonstration of point-to-multipoint coherent transmission for 5G mobile transport over existing fiber plant,” in *Proc. of ECOC 2021*, pp. 1–4, Sept. 2021.
- [40] H. Shakespear-Miles, M. Ruiz, A. Napoli, and L. Velasco, “Dynamic subcarrier allocation for multipoint-to-point optical connectivity,” in *Proc. of OECC/PSC 2022*, pp. 1–4, Jul. 2022.
- [41] S. Ramamurthy, L. Sahasrabudde, and B. Mukherjee, “Survivable WDM mesh networks,” *J. Lightw. Technol.*, vol. 21, pp. 870–883, Apr. 2003.
- [42] R. Proietti *et al.*, “Experimental demonstration of machine-learning-aided QoT estimation in multi-domain elastic optical networks with alien wavelengths,” *J. Opt. Commun. Netw.*, vol. 11, pp. A1–A10, Jan. 2019.
- [43] M. Liu, M. Tornatore, and B. Mukherjee, “Survivable traffic grooming in elastic optical networks - shared protection,” *J. Lightw. Technol.*, vol. 31, pp. 903–909, Mar. 2013.
- [44] X. Liu, L. Gong, and Z. Zhu, “Design integrated RSA for multicast in elastic optical networks with a layered approach,” in *Proc. of GLOBECOM 2013*, pp. 2346–2351, Dec. 2013.
- [45] “Detailed Release Notes for Gurobi 9.5.2.” [Online]. Available: https://www.gurobi.com/documentation/9.5/refman/detailed_release_notes_for.html